

Sensor Validation and Fusion for Gas Turbine Vibration Monitoring

Weizhong Yan⁺ and Kai Goebel^{*}
GE Global Research Center

ABSTRACT

Vibration monitoring is an important practice throughout regular operation of gas turbine power systems and, even more so, during characterization tests. Vibration monitoring relies on accurate and reliable sensor readings. To obtain accurate readings, sensors are placed such that the signal is maximized. In the case of characterization tests, strain gauges are placed at the location of vibration modes on blades inside the gas turbine. Due to the prevailing harsh environment, these sensors have a limited life and decaying accuracy, both of which impair vibration assessment. At the same time bandwidth limitations may restrict data transmission, which in turn limits the number of sensors that can be used for assessment. Knowing the sensor status (normal or faulty), and more importantly, knowing the true vibration level of the system all the time is essential for successful gas turbine vibration monitoring. This paper investigates a dynamic sensor validation and system health reasoning scheme that addresses the issues outlined above by considering only the information required to reliably assess system health status. In particular, if abnormal system health is suspected or if the primary sensor is determined to be faulted, information from available “sibling” sensors is dynamically integrated. A confidence expresses the complex interactions of sensor health and system health, their reliabilities, conflicting information, and what the health assessment is. Effectiveness of the scheme in achieving accurate and reliable vibration evaluation is then demonstrated using a combination of simulated data and a small sample of a real-world application data where the vibration of compressor blades during a real time characterization test of a new gas turbine power system is monitored.

Keywords: Sensor Validation; Diagnostics; Information Fusion; Data Fusion; Simulation, Monitoring, Vibration;

1. INTRODUCTION

Compressor blades and turbine buckets of gas turbines are subjected to high cycle fatigue (HCF) failure. To prevent the HCF failures, the vibratory stresses of these blades or buckets are carefully monitored during a factory characterization test of a new gas turbine system. Vibration monitoring has two primary functional purposes: 1) it allows for validating the system design and 2) it serves as a means to prevent possible excessive vibration induced damage to the system components. For fulfilling these two goals, reliable and accurate sensor readings of vibration is imperative.

Blade or bucket vibration is typically of high frequency and exhibits a multitude of modes. Strain gauges attached to the surface of blades or buckets are often used for measuring the vibration level. Due to the nature of high frequency vibration and the harsh environment inside gas turbines, sensors are prone to fail or to give erroneous readings. Suspicious or erroneous sensor readings may result in unnecessary turbine “trips”, i.e., the run is aborted. This results in a longer test time, which in turn increases the testing cost. More importantly, faulty sensors may issue readings that could mask true excessive vibration, thus preventing detection of impending damage to the system. Knowing the true vibration level of the system all the time through effective validation of sensor reading is, therefore, essential and required in general for successful gas turbine vibration monitoring, and in particular for successful factory characterization tests.

Sensor validation can be accomplished through either hardware or software redundancy. For gas turbine blade vibration monitoring, using redundant sensors would not only require more sensors and more data acquisition equipment, but would also mean more channels of signals that need to be transmitted through the telemetry system. The telemetry is a bottleneck for gas turbine factory tests due to the competition for limited space in the shaft of the gas turbine. Where

⁺ yan@research.ge.com; phone 1 518 387-5704; fax 1 518 387-6104; GE Global Research, K1-5B34B, 1 Research Circle, Niskayuna, NY 12309, USA

^{*} goebelk@research.ge.com; phone 1 518 387-4194; fax 1 518 387-6104; <http://best.me.berkeley.edu/~goebel/kai.html>; GE Global Research, K1-5C4A, 1 Research Circle, Niskayuna, NY 12309, USA

data need to be transmitted to a remote monitoring site, additional restrictions are imposed on data transmission due to bandwidth limitations

This paper investigates a dynamic sensor validation and system health reasoning scheme that intelligently integrates the sensor readings from the sensor in question and – if required because either abnormal system health is suspected or the primary sensor has gone bad – those from available “sibling” sensors as well. Sibling sensors are defined to be placed at a location that has a mechanical correlation to the sensor in question. The scheme determines the health of sensors and integrates only information from validated sensors. We show how system health assessment can be accomplished in an environment where any sensor can fail unpredicted.

Section 2 provides an overview of sensor validation and sensor fusion techniques. Section 3 describes the technical approach, specifically the feature extraction and confidence estimation. Section 4 demonstrates results from tests performed and section 5 concludes with a discussion and final remarks.

2. BACKGROUND

Sensor Validation

A large number of sensors are used during the characterization tests of a gas turbine. These include thermo couples, pressure sensors, mass flow rate sensor and the engine speed sensor as well as strain gauges that are mounted on blades and buckets. These strain gauges are not expected to last very long due to the severe local environmental conditions. In addition, they are impractical for prolonged use due to technical hurdles surrounding the telemetry. It is therefore crucial to determine whether a sensor is still producing valid results or not. It is even more important to distinguish between sensor failure and system malfunction. A sensor validation scheme should fulfill the tasks of detection and diagnosis. The former involves discovering a malfunction in a sensor while the latter can be subdivided into three stages: localization (establishing which sensor has failed), identification, and estimation¹. Given the vast number of different sensors used, the sensor validation methodology needs to be flexible enough to accommodate the different sensor configurations that are dynamically changing due to the sensors that could fail unpredicted.

Limit checking is one of the classical methods of checking the sensory data for outliers. The Algorithmic Sensor Validation (ASV) filter² compares the difference between the sensor readings and the validated reading at the previous sampling time to the maximum possible change that is possible. This maximum change can be obtained by looking at the physical constraints of the system. For sensors whose output can be captured by a model, techniques such as Kalman filtering can be used to create a validation gate that is the measurement space where the measurement will be found with some (high) probability³. Measurements that lie within the gate are considered valid while those outside are too far from the expected location and thus are unlikely. Variants of this principle are fuzzy validation gates⁴.

Sensor values can be validated through comparisons with redundant measurement values. The redundancies of the sensors can be characterized into two types: *spatial redundancy* and *temporal redundancy*. The spatial redundancy of a sensor can be obtained through a redundant sensor or through a functional and logical relationship among the parameter values measured by different sensors. The redundancy obtained by functional relationship is often called analytic redundancy of which the parity space approach is a good example^{5 & 6}. Temporal redundancy of a sensor value is obtained by repetitive measurements of the sensor values at regular intervals. For sensors without direct redundancy but related with a group of sensors in a subsystem, the probabilistic approach of maximum a posteriori (MAP) can be used. Here, a multivariate Gaussian distribution for the sensor output is assumed and the sensor output is compared to the parameter value that maximizes the probability distribution². More recently, neural networks⁷ and kernel-based techniques⁸ have also been used for modeling the relationship between sensors that are not direct redundant, but are related for sensor validation purpose.

The validation scheme should also be able to check for other sensor faults such as sensor bias, and drift. Complete malfunction (failure) of the sensors is relatively easy to detect, but when complete failure occurs, it can lead to catastrophic events. Therefore, it is imperative to detect latent malfunctions in the sensor to predict the degradation in sensor performance. To that end a sliding window can be used. The statistical properties of the measurement residue (difference between the sensor output and the fused estimated value of the parameter) can be used for this process. It is relatively simple to check for sensor bias when multiple sensors are present. The measurement residue ideally should be zero mean, white and Gaussian. An estimate of the sensor bias can be obtained by looking at the mean of measurement

residue over a number of sliding windows. If the mean is non zero and remains constant then it can be attributed to the bias in the sensor. This can be checked by a test of hypothesis that there is a change in the mean of measurement noise over successive sliding windows⁹. The measurement residue can also be tested for whiteness and for variance^{10, 11, & 12}.

To detect slow variations in the sensor performance the drift test can be carried out periodically off-line⁹. For this a steady state test which aims at determining whether the examined variables are in static or dynamic state is carried out. For the drift test, the steady state test is first carried out for two different windows: small and large. If the steady state test (utilizing the small window) detects a steady state for a duration equal to the large window and if for the same duration the steady state test (utilizing the large window) detects a dynamic state, then a drift is present.

Data Fusion

Most single sensors cannot be relied on to deliver (acceptably) accurate information all the time. Further, associated with any sensor is a set of limits that define its useful operating range. Unless these are taken into account incorrect inferences might be drawn. Sensor signals are also inevitably corrupted by noise. Even when two or more sensors are operating within their limits they may deliver results at the opposite end of the valid region. Fusing their measurements can provide a more robust or reliable reading than that provided by any one sensor because signals tend to be correlated between sensors whereas noise is uncorrelated.

The potential advantages of the synergistic use of multi-sensor information can be decomposed into four fundamental aspects: 1) redundancy: reduced uncertainty and increased reliability in case of sensor error or failure, 2) complementary information: multiple sensors allow features in the environment to be acquired using just the information from each individual sensor operating separately, 3) timeliness: more timely information is obtained compared to the speed at which it would be provided by a single sensor due to either the actual speed of operation of each sensor, or the processing parallelism that may be achieved as a part of the integration process, and 4) less costly information: in the context of a system with multiple sensors information may be obtained at a lesser cost when compared to equivalent information that could be obtained from a single sensor¹³. It is therefore desirable to have a methodology for fusing data obtained from diversified sources in a coherent fashion.

Data fusion has been tackled by several different methods. One of the simplest and intuitive general methods of fusion is to take a weighted average of redundant information provided by a group of sensors and use this fused value. The Kalman filter can be used to fuse low-level redundant data in real time by taking advantage of the statistical characteristics of the measurement model to determine estimates recursively for the fused data that are optimal in a statistical sense. In Bayesian estimation using consensus sensors¹⁴, sensor information that is likely to be in error is eliminated and the information for the other 'consensus sensors' is used to calculate the fused value. The information from each sensor is represented as a probability density function and the optimal fusion of the information is determined by finding the Bayesian estimator that maximizes the likelihood function of the consensus sensors. Durrant-Whyte¹⁵ uses a multi-Bayesian approach, where each sensor is considered as a Bayesian estimator, to combine the associated probability distributions of each respective feature into a joint posterior distribution function. A likelihood function of this joint distribution is then maximized to provide the final fusion of the sensory information. In statistical decision theory^{16 & 17}, data from different sensors are subject to a robust hypothesis test as to its consistency. Data that pass this preliminary test are then fused using a class of robust minimax decision rules. Dempster-Shafer evidential reasoning¹⁸, an extension of the Bayesian approach, makes explicit any lack of information concerning a proposition's probability by separating firm support for the proposition from just its plausibility. Fuzzy Logic¹⁹ used for data fusion allows the uncertainty in the multisensor fusion to be directly represented in the fusion (inference) process by allowing each proposition, as well as the actual implication operator, to be assigned a real number from 0 to 1 to indicate its degree of truth. Production rule based systems²⁰ are used to represent symbolically the relation between an object feature and the corresponding sensory information. A confidence factor is associated with each rule to indicate its degree of uncertainty. Fusion takes place when two or more rules are combined during logical inference to form one rule.

3. TECHNICAL APPROACH

3.1 Overall architecture

In this approach we perform sensor validation and system health reasoning by taking advantage of a host of information. The information sources include strain gauge readings and extracted features, design limits, alarm

thresholds, strain gauge position (turbine section, blade, position on blade), and position of related strain gauges (“sibling sensors”). The process flow of the sensor validation and the system health reasoning is as follows (Figure 1): For each channel of interest, find all channels at the same turbine section on either the same blade but different position or a different blade. Next, extract features both in the frequency and time domains. These features are then (after a down-selection process) fed into a classifier. The output of the classifier is the sensor health status.

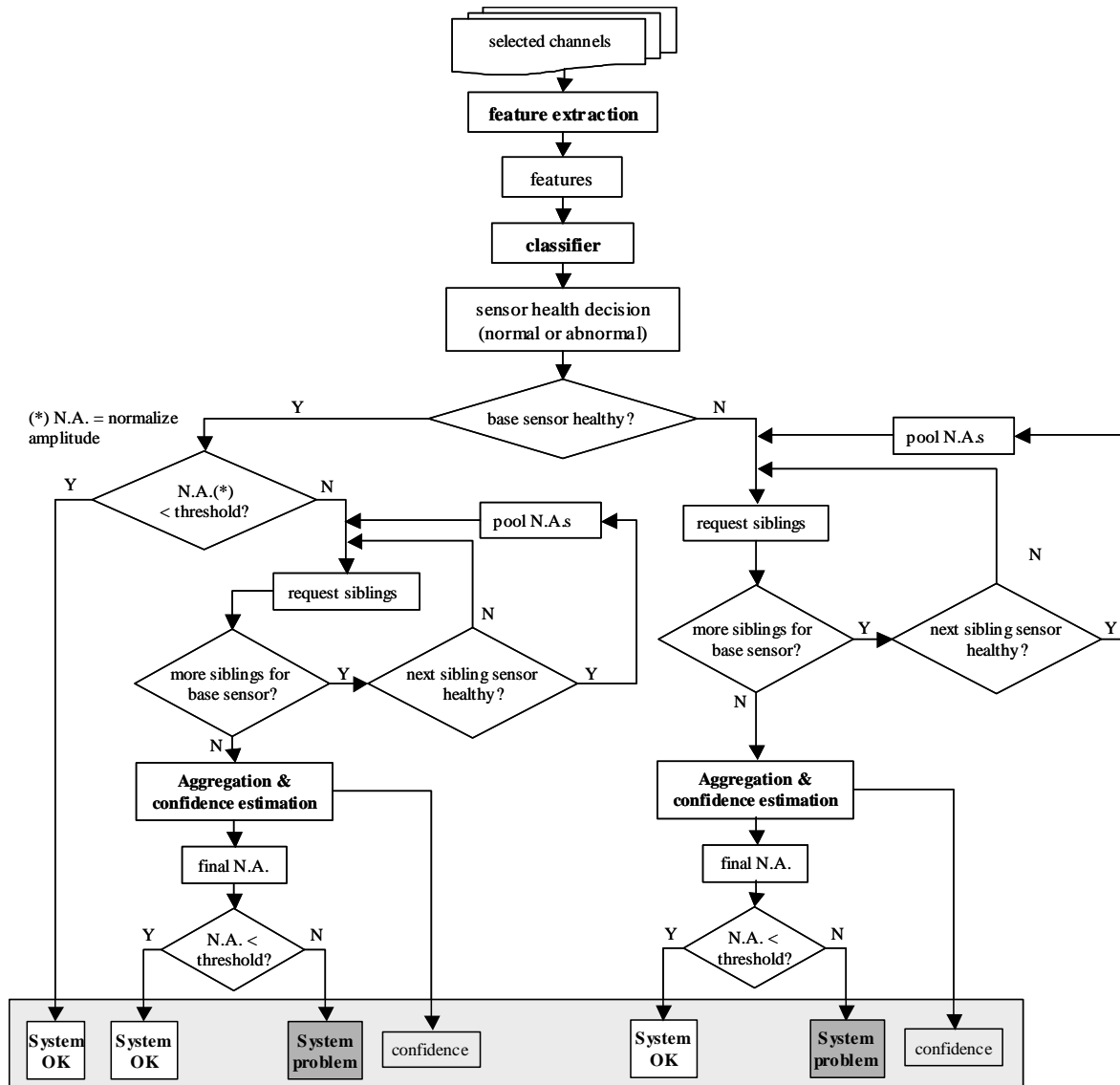


Fig. 1: Sensor validation and system health reasoning process map

After that, system health is evaluated. In this case, system health means the vibration status (i.e., whether or not the vibration is over the design limit) of the blade or bucket monitored. Initially, there is a check whether the sensor readings fall above an alarm threshold. If it does not, the system is evaluated as working properly. If the threshold is surpassed, confirmatory information is requested from associated sensors (“sibling” sensors). If these pass the health test, their normalized amplitudes are aggregated to arrive at a final system health status and its associated confidence is also estimated. If the base sensor was judged to be not healthy, system health still needs to be evaluated. In that case, only healthy sibling sensors are used for evaluation using the procedure described above.

3.2 Feature extraction

Just like in any fault diagnosis, feature extraction is an important step in detecting sensor faults. Feature extraction is essentially to find the characteristics of the sensor signals, which can be used to distinguish faulty sensors from healthy sensors. For a typical vibration signal analysis, features can be extracted from both frequency and time domains. For the gas turbine characterization test under investigation, data analysis takes place at a remote location, which means there are rather strict limitations on data transmission size. To ease the bandwidth restrictions, only frequency components of the sensed signals were transmitted. Therefore, this study examines only frequency domain features. In particular, we use primarily basic shape statistics as features to characterize a spectrum for sensor fault detection purpose. The shape statistics include the centroid, the standard deviation, the skewness, and the kurtosis. Assuming f_i and A_i are the i^{th} mode frequency and amplitude, respectively, of a spectrum, the shape statistics of the spectrum are defined as follows ²¹.

$$\text{Centroid: } C = \frac{\sum_{i=1}^N A_i \cdot f_i}{\sum_{i=1}^N A_i} \quad (1)$$

$$\text{Standard deviation: } S = \sqrt{\frac{\sum_{i=1}^N (f_i - C)^2 \cdot A_i}{\sum_{i=1}^N A_i}} \quad (2)$$

$$\text{Skewness: } S_k = \frac{\sum_{i=1}^N (f_i - C)^3 \cdot A_i}{S^3 \cdot \sum_{i=1}^N A_i} \quad (3)$$

$$\text{Kurtosis: } K_t = \frac{\sum_{i=1}^N (f_i - C)^4 \cdot A_i}{S^4 \cdot \sum_{i=1}^N A_i} \quad (4)$$

Another important feature is the normalized amplitude at each of the vibration modes. The vibration modes of a turbine blade are the engineer's predictions, which may not exactly match the real vibration modes, due to modeling error, manufacturing tolerances, etc. To account for these uncertainties, we allow some slack in the description of the vibration mode which will permit readings "in the neighborhood" of the designed frequency mode to be counted towards the feature (Figure 2). Let $\{f_i, A_i\}, i = 1, \dots, n$ be the first n predicted vibration modes (where n is in this specific case a number around one dozen). The corresponding vibration modes with slack would be $\{f_i \pm \Delta_f, A_i^*\}, i = 1, \dots, n$, where Δ_f is the half width of the "neighborhood" bin and A_i^* is the maximum amplitude of all vibration modes inside the i^{th} bin. The normalization takes place with respect to the predicted design limit of amplitude at the respective frequency mode.

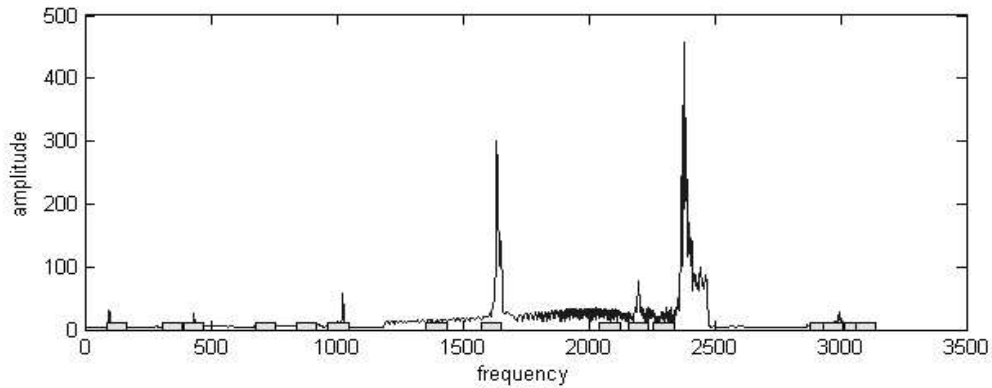


Fig. 2: Vibration mode bins

3.3 Classification

For the sensor fault detection case here, classification means the decision on whether the sensor performs normally or abnormally based on the extracted features. There are a variety of classifiers, ranging from statistics-based methods to those using soft computing technology, which can be used for sensor fault detection. Due to the fact that the specific problem offered only few examples and the desire for a simple design with high interpretability, we use rule based decision tree as the classifier. As fine-tuning performance becomes a bigger issue and more test cases (for both normal and faulty sensors) become available, more sophisticated classifiers may be chosen.

3.4 Aggregation

The outputs of the individual healthy sensors are aggregated to arrive at the final decision about system health. Depending on the health status of the base sensor and the number of healthy “sibling” sensors, the aggregation is performed “dynamically” as indicated in the system health reasoning process map in Figure 1. The final composite amplitude representing the vibration level of the blade monitored is the maximum of the normalized amplitudes of all healthy sensors. System health status is then determined by comparing the composite amplitude against the pre-defined alarm threshold.

3.5 Confidence estimation

As a further decision support aid, confidence associated with the predicted status is estimated and provided to the engineers. The confidence of the system health status varies depending on the following factors:

- 1) Number of healthy sensors available,
- 2) Different levels of preference/reliability of sensors at different locations,
- 3) Degree of closeness in sensor outputs,
- 4) Degree of conflict in sensor outputs,
- 5) Magnitude of the normalized amplitude.

In this study, we propose a confidence estimation method that is based on empirical quantification of each of the above-mentioned factors. The confidence, C , associated with a predicted system health status is calculated as

$$C = C_b \cdot \alpha \cdot \beta \cdot \gamma \quad (5)$$

where, $C_b \in [0,100]$ represents the base confidence reflecting the number of healthy sensors available and reliability levels of different sensors (factors 1 and 2 above); $\alpha \in [0.75,1.0]$, $\beta \in [0.0,1.0]$, and $\gamma \in [0.9,1.0]$ are the three confidence reduction factors representing factors 3, 4, and 5, respectively. A brief description of the four parameters of Equation 5 is given below.

Base confidence C_b

The number of healthy sensors available is an important factor in confidence determination. Without considering conflicting and other factors, more healthy sensors generally yield a more reliable measurement of the true vibration level, thus higher confidence on system health condition reasoning. For gas turbine characterization test, the reasoning is performed typically based on three different sensors. Sensor 1 is defined as the base or primary sensor located at the location of interest on the blade. Sensor 2 is defined to be located at the same position as sensor 1, but at different blade of the same stage. Sensor 3 is defined as located at a different position of the same blade as sensor 1. To capture the notion that more healthy sensors available lead to a higher confidence, we assign different levels of base confidence for different number of healthy sensors, e.g., 100% if all three are healthy, 75% if only two sensors are healthy, and 50% if only one sensor is healthy. Also, we would expect different relevance for the three sensors to the query posed. We prefer sensor 1 the most since it is located at the location of interest. We also prefer sensor 2 over sensor 3 since the location of sensor 2 is structurally similar to that of sensor 1 while sensors 3 and 1 are only correlated via analytical relationship. Based on the number of sensors and individual sensor preference, the base confidence is assigned as shown in Table 1. This base confidence is the maximally possible confidence level for the specific sensor combination because several discounting factors are employed. For example, when only two sensors (sensors 1 & 3) are available (case # 3 in the table), the maximum confidence is 75%. If only one healthy sensor is available, the maximum confidence varies from 55% to 45%, depending on which sensor (1, or 2, or 3) is available.

Table 1: Base confidence assignment

Case #	Sensor 1	Sensor 2	Sensor 3	Confidence C_b
1	+	+	+	100%
2	+	+	0	85%
3	+	0	+	75%
4	0	+	+	65%
5	+	0	0	55%
6	0	+	0	50%
7	0	0	+	45%
8	0	0	0	0%

Note: “+” in the table indicates a healthy sensor while “0” indicates a bad sensor.

Degree of closeness α

Degree of closeness is used to capture the support among the healthy sensors when more than one sensor indicates an over-the-limit vibration. We will demonstrate this using two illustrative example cases. The normalized amplitudes given by three sensors are [0.85, 0.86, 0.85] for case A and [0.95, 0.86, 0.76] for case B. Let the alert threshold Th be 0.75. All three sensors in both cases give the same indication that the system vibration is over the limit. However, in case A all three numbers are almost identical (more supportive) while the three numbers in case B are much more different (less supportive). The close outputs from the individual sensors of case A lead to a higher confidence for the final decision on system health. Thus, the degree of closeness factor is proposed to be a function of the maximum difference among the normalized amplitudes of the individual sensors. A function capturing this relationship can be defined as:

$$\alpha = T_1 - \frac{1}{e^{-15\delta_{\max} + T_2}} \quad (\delta_{\max} \in [0, 1 - Th]) \quad (6)$$

Where, T_1 and T_2 are empirically determined tuning parameters (here, $T_1=1.006$ and $T_2=5.136$); Th is the pre-defined limit threshold; δ_{\max} is the maximum difference among the normalized amplitudes. For the 2 example cases given above, δ_{\max} is 0.01 and 0.19 for cases A and B, respectively. α attains maximum value of 1.0 when all available sensors give exactly the same value of normalized amplitudes. α is set to 1.0 when only one healthy sensor is available or only one sensor shows the over-the-limit vibration. There is also a minimum value for α (here, $\alpha = 0.75$) to limit the confidence reduction.

Degree of conflict β

We frequently encounter conflicting indications from different sensors. That is, one sensor indicates an over-the-limit vibration while another sensor shows that the vibration is below the limit. The conflicts would certainly adversely affect our confidence on our final decision on the vibration status of the system, i.e., the higher the degree of the conflict is, the lower the confidence will be. Again we will use two illustrative examples (Figure 3). In both cases (cases A and B), sensor 1 has normalized amplitude of 0.9, exceeding the specified design limit of 0.75, while sensor 2 in both cases indicates a below-the-limit vibration. However, in case A, sensor 2 has amplitude of 0.7, which is slightly below the design limit of 0.75. In case B, on the other hand, sensor 2 has the amplitude of 0.2, which is much below the limit. Case B has obviously more severe conflict than case A does and a larger confidence reduction for case B should be expected. We propose a degree of conflict to capture this notion. The degree of conflict factor, β , is defined as a function of the maximum difference of the amplitudes between the conflicting sensors, as shown in Equation 7.

$$\beta = (1 - \Delta^{T_3})^{\frac{1}{3}} \quad (\Delta \in [0, 1]) \quad (7)$$

where, Δ is the maximum difference of the amplitudes between two conflicting sensors, T_3 is a tuning parameter (here $T_3 = 1.8$).

The degree of conflict factor, β , has a maximum value of one, which indicates a no-conflict situation. β can be close to zero, but can never be equal to zero since Δ can not be 1 ($\Delta=1$ indicates a bad sensor).

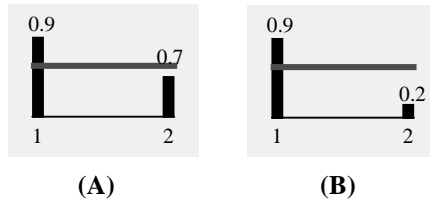


Fig. 3: Two examples

Level of magnitude γ

When estimating confidence, we also take into account the absolute magnitude of the normalized amplitudes of the sensors. We slightly lower the confidence for the higher magnitude of the final predicted vibration level. The reason behind this is that higher magnitude more likely leads to a more critical decision, i.e., vibration exceeded or not, or even more critical decision on if the system will be tripped or not. Similar to the other two factors, the level of magnitude factor, γ , is expressed as a function of the normalized amplitude, A_n as in Equation 8.

$$\gamma = T_4 - \frac{1}{e^{(-3A_n + T_5)}} \quad (A_n \in [0, 1]) \quad (8)$$

where, T_4 and T_5 are the tuning parameter (here $T_4=1.005$ and $T_5=5.25$). γ has a value range from 0.9 to 1.0.

Figure 4 shows the function curves of the three confidence reduction factors, α , β , and γ .

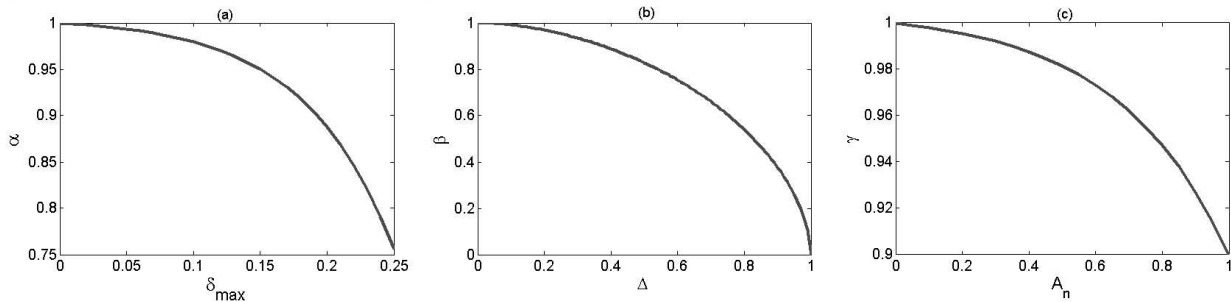


Fig. 4: The three confidence reduction factor curves; a.) α ; b.) β ; c.) γ

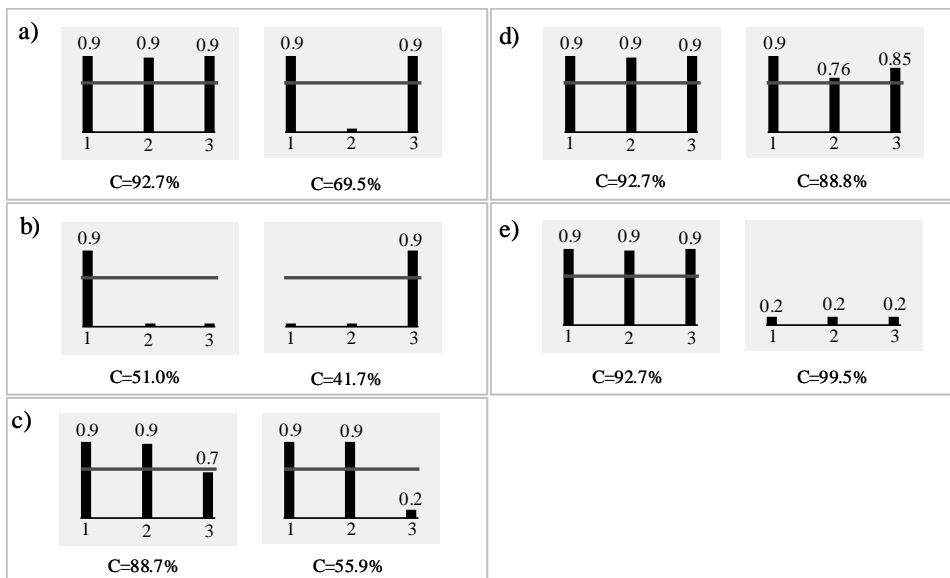


Fig. 5: Confidence comparison for representative cases

To illustrate that the confidence estimation method indeed addresses all of the 5 issues (number of healthy sensors available, different levels of preference/reliability of sensors at different locations, degree of closeness in sensor outputs, degree of conflict in sensor outputs, and magnitude of normalized amplitude), we have calculated the confidence value for a number of representative cases as shown in Figure 5, where the normalized amplitudes of the three sensors are shown for each case (horizontal bar represents the alarm threshold). There are 5 subplots in Figure 5, each of which has two cases. By comparing the sensor outputs and the calculated confidence values (C in the figure) of the two cases in each subplot, one can appreciate how different factors affect the confidence value. For example, subplot 1 shows the effect of number of healthy sensors. The two cases in subplot 1 indicate that when one of the sensors (sensor 2) fails, the confidence value reduces from 92.7% (case 1) to 69.5% (case 2), although the outputs for the other 2 sensors remain unchanged. Similarly, subplots 2 through 5 are for the factors of different levels of preference of sensors at different locations, degree of closeness, degree of conflict, and level of magnitude, respectively.

4. APPLICATION

We applied the sensor validation and system health reasoning scheme to vibration monitoring during a factory characterization test of a gas turbine. At the time of publication, only a small sample of data from initial test runs is available which we will use to demonstrate the effectiveness of the sensor fault detection. For system health reasoning, we have to rely on simulated cases to test the confidence estimation method.

Figure 6 shows the spectrum waterfalls of 2 correlated sensors that are placed at the same location of different blades. Both sensors are in normal (fault-free) condition. As the turbine speed increases, the vibration frequency changes linearly as indicated by the diagonal frequency band. Vibration amplitude and frequency components are very similar between the two sensors. Figures 7 and 8 show the normalized amplitude waterfalls and peak-holds, respectively, for the same two sensors under fault-free condition. Once again, both normalized amplitude waterfalls and the peak-holds show strong similarity between the two sensors. However, when one of the two sensors fails during the middle of the test, the normalized amplitude waterfalls (Figure 9) and the peak-holds (Figure 10) of the two sensors show noticeable differences. The shape statistics based features and the normalized amplitudes effectively detect the sensor failure.

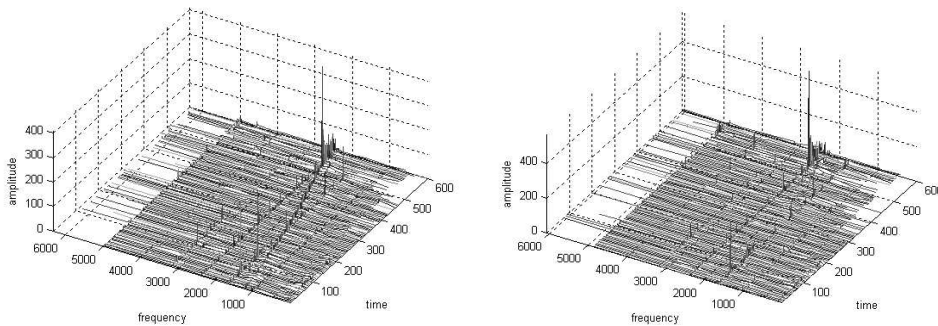


Fig. 6: Spectrum waterfalls for two correlated sensors under fault-free condition

Figure 11 shows the simulation results of the system health reasoning. Each dot or circle in the figure indicates one case. Sensors 2 and 3 have three condition statuses, i.e., sensor is bad, vibration is over the limit, and vibration is below the limit, while Sensor 1 only has two condition statuses, i.e., sensor is bad and vibration is over the limit. A total of 85 cases are generated to cover all different combinations of the condition statuses of the three different sensors. The outputs (normalized amplitudes) of each sensor are randomly generated. Figures 11(a) through 11(c) show the normalized amplitudes for three correlated sensors, respectively, where zeros in the value indicate faulty sensors (sensors values were set to zero after a sensor fault is detected). Figure 11(d) shows the outputs of the system health reasoning after aggregation of the sensor outputs. Figure 11(e) shows the confidence calculated using the proposed method. It can be seen that the first 45 cases of the simulation generally have higher estimated confidence than the rest of the cases. This is because the base sensor (sensor 1) is healthy for the first 45 simulation cases and went to bad afterwards. One can also see from the figure that the estimated confidence value drops whenever conflicting outputs

between healthy sensors occur (Cases 6, 8, 13, 18, 26, and 51). In particular, Case # 26 has the lowest confidence estimated. Here, sensor 3 is faulty while sensors 1 and 2 have the outputs (normalized amplitudes) of 0.97 and 0.03, respectively, which is close to the most severely conflicting situation, thus yielding a lowest confidence.

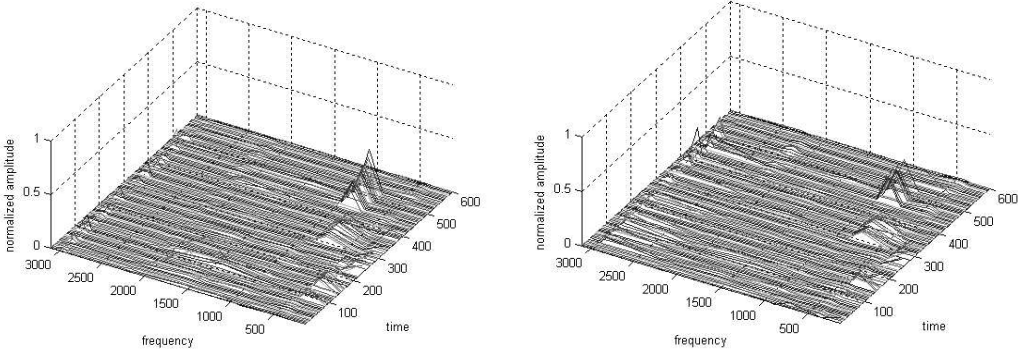


Fig. 7: Normalized amplitude waterfalls for two correlated sensors under fault-free condition

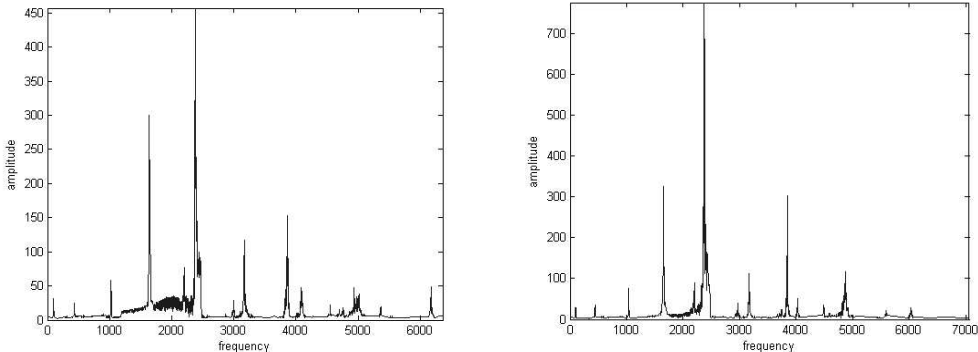


Fig. 8: Peak-holds for two correlated sensors under fault-free condition

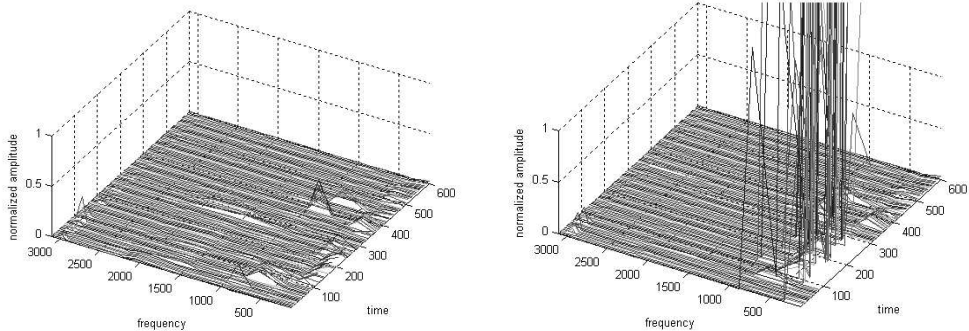


Fig. 9: Normalized amplitude waterfalls for two correlated sensors when 2nd sensor fails

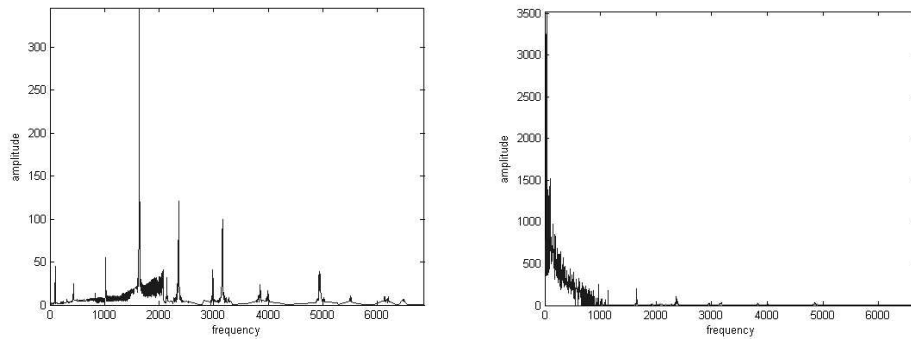


Fig. 10: Peak holds for two correlated sensors when 2nd sensor fails

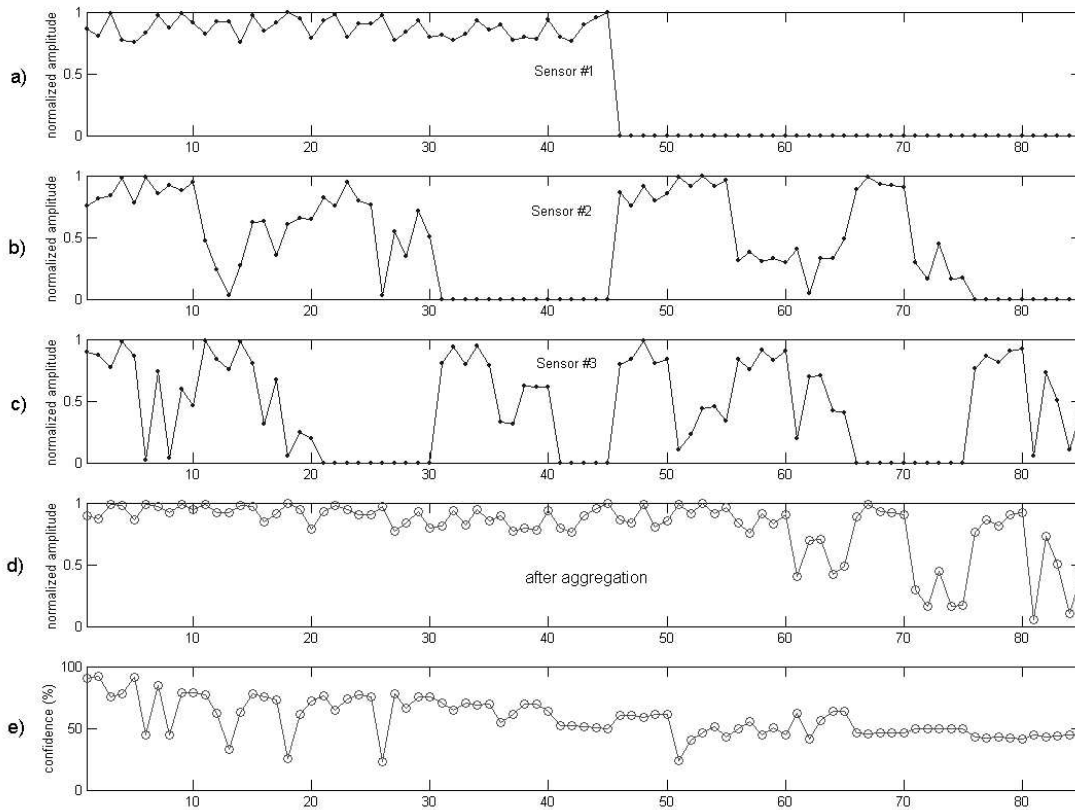


Fig. 11: Simulated results for system health reasoning; a.) sensor 1; b.) sensor 2; c.) sensor 3; d.) aggregated output; e.) aggregated confidence

5. SUMMARY AND CONCLUSIONS

This paper introduced a sensor validation and system health reasoning scheme that integrates sensor readings from the primary sensor and those from available “sibling” sensors. The sibling sensors are not directly redundant sensors but are sensors that are placed at a location that is mechanically correlated to the location of the primary sensor. Due to bandwidth limitations, not all sensors can be used at all times for validation. Rather, additional information will be

polled when suspicious behavior is encountered. In particular, additional information is requested when the primary sensor malfunctions or when abnormal system behavior is encountered. Malfunction of the primary sensors is indicated by a classifier that uses statistical shape features to perform classification. A confidence measure expresses the degree of closeness, the degree of conflict, and the level of magnitude in relation to the alarm threshold of the overall health assessment.

Future work should expand the proposed scheme to cases without bandwidth limitation. It is expected that a continuous confirmation of sensors lead to even higher fidelity of system health assessment. In general, there are a number of other information sources available that could also be used to refine the estimated system status. This information includes inlet guide vane position, exhaust gas temperature, etc.

REFERENCES

1. Bar-Shalom, Y., editor. *Multitarget-Multisensor Tracking: Advanced Applications*. Artech House, Norwood, MA, 1990.
2. Kim, Y.J., W.H. Wood, and A.M. Agogino, "Signal Validation for Expert System Development," *Proceedings of the 2nd International Forum on Expert Systems and Computer Simulations in Energy Engineering*, March 17-20, 1992 (Erlangen, Germany), pp. 9-5-1 to 9-5-6.
3. Bar-Shalom, Y. and T. E. Fortmann, *Tracking and Data Association*. Boston, MA: Academic, 1988.
4. Goebel, K. and Agogino, A., "Fuzzy Sensor Fusion of Gas Turbine Power Plants", *Proceedings of SPIE, Sensor Fusion: Architecture, Algorithms, and Applications III*, Vol. 3719, pp. 52-61, 1999.
5. Chew, E. Y. and Wilsky, A. S., "Analytic Redundancy and the Design of the Robust Failure Detection System", *IEEE Trans. Auto. Contr.*, vol. AC-29, pp. 603-614, July 1984.
6. Lee, S. C., "Sensor Value Validation Based on Systematic Exploration of the Sensor Redundancy for Fault Diagnosis KBS", *IEEE Transactions on Systems, Man and Cybernetics*, vol. 24, no. 4, April 1994.
7. Mattern, D. L., Jaw, L.C., Guo, T-H, Graham, R. and McCoy, W., "Using Neural Networks for Sensor Validation", NASA Report (Number: NASA TM-1998-208484), National Aeronautics and Space Administration, Washington, DC 20546-0001.
8. Gribok, A.V., Hines, J.W., and Uhrig, R.E., "Use of Kernel Based Techniques for Sensor Validation in Nuclear Power Plants", The 3rd American Nuclear Society International Topical Meeting on Nuclear Plant Instrumentation, Controls, and Human-Machine Interface Technologies, Washington, DC, November 13-17, 2000.
9. Pouliezos A. D. and G. S. Stavrakankis, *Real Time Fault Monitoring of Industrial Processes*. Kulwer Academic Publishers, Dordrecht, 1994.
10. Kendall M. Stuart A. and J. k. Ord, *The Advanced Theory of Statistics*. vol. 2 and 3. Charles Criffin Ltd., London, 1982.
11. Anderson T. W., *An Introduction to Multivariate Statistical Analysis*. John Wiley, New York, 1958.
12. Bennett C. A. and N. L. Franklin. *Statistical Analysis in Chemistry and the Chemical Industry*. John Wiley, 1954.
13. Luo, R. C. and Kay, M. G., "Multisensor Integration and Fusion in Intelligent Systems", *IEEE Transactions on Systems, Man, and Cybernetics*, vol. 19, no. 5, 1989.
14. Lou, R. C. and Lin, M., "Dynamic multi-sensor Data Fusion system for Intelligent Robots", *IEEE J. Robot. Automation.*, vol. RA-4, no. 4, pp. 386-396, 1988.
15. Durrant-Whyte, H. F., "Consistent Integration and Propagation of Disparate Sensor Observations," *INT. J. Robot. Res.*, vol. 7, no. 6, pp. 97-113, 1988.
16. Zeytinoglu, M. and Mintz, M., "Robust Fixed Sized Confidence Procedure for a Restricted Parameter Space", *Ann. Statist.*, vol. 16, no. 3, pp. 1241-1253, 1988.
17. Kim, Y.J., "Uncertainty Propagation in Intelligent Sensor Validation," Ph.D. dissertation, University of California, Berkeley, CA, Spring 1992.
18. Shafer, G., *A Mathematical Theory of Evidence*, Princeton, NJ, Princeton Univ. Press, 1976.
19. Zadeh, L. A., "Fuzzy Sets", *Inform. Contr.*, vol. 8, pp. 338-353, 1965.
20. Kamat, S. J., "Value Function Structure for Multiple Sensor Integration", *Proc. SPIE*, vol. 579, *Intell. Robots and Computer Vision*, Cambridge, MA, Sept. 1985.
21. Winkler, R. L. and Hays, W. L., *Statistics: Probability, Inference, and Decision*, 2nd Edition, Chapter 3, Holt, Rinehart and Winston, 1975.